

Article

Solventless Coupling of Epoxides and CO₂ in Compressed Medium Catalysed by Fluorinated Metalloporphyrins

Rui M. B. Carrilho^{1,2}, Lucas D. Dias¹, Raquel Rivas², Mariette M. Pereira^{1,*}, Carmen Claver^{2,3} and Anna M. Masdeu-Bultó^{2,*}

¹ CQC, Department of Chemistry, University of Coimbra, Rua Larga, 3004-535 Coimbra, Portugal; rui.carrilho@uc.pt (R.M.B.C.); lucasdanillodias@gmail.com (L.D.D.)

² Department of Physical and Inorganic Chemistry, University Rovira i Virgili, Marcel·lí Domingo, Tarragona 43007, Spain; raquel.rivas@urv.cat (R.R.); carmen.claver@urv.cat (C.C.)

³ Centre Tecnològic de la Química, Marcel·lí Domingo s/n, Campus Sescelades, Tarragona 43007, Spain

* Correspondence: mmpereira@qui.uc.pt (M.M.P.); annamaria.masdeu@urv.cat (A.M.M.-B.); Tel.: +351-239-854-474 (M.M.P.); +34-977-558-779 (A.M.M.-B.)

Received: 22 June 2017; Accepted: 7 July 2017; Published: 14 July 2017

Abstract: Metal complexes of *meso*-arylporphyrins (Cr(III), Fe(III), and Zn(II)) were evaluated in the coupling reaction of cyclohexene oxide (CHO) with CO₂ in compressed medium, where the Cr complexes were demonstrated to be the most active systems, leading predominantly to copolymerisation products. It is noteworthy that no addition of solvent was required. To improve the catalytic activity, and to simultaneously increase the solubility in compressed CO₂, a new fluorinated catalyst, tetrakis(4-trifluoromethylphenyl)porphyrinatochromium(III) chloride (CrCl-*p*CF₃TPP), was applied to this reaction. The alternating copolymerisation of CHO with CO₂, using the Cr(III) fluorinated porphyrin catalyst, required the use of a co-catalyst, bis(triphenylphosphine)iminium chloride (PPNCl), with the best yields of copolymers being obtained at 80 °C, and CO₂ pressures in the range of 50–110 bar, over a period of 24 h, with a low catalyst/substrate molar ratio (0.07%). The polycarbonate's structure was analysed by ¹H NMR, ¹³C NMR, and MALDI-TOF spectroscopy, which demonstrated high carbonate incorporations (98–99%). Gel permeation chromatography revealed number-average molecular weights (*M_n*) in the range of 4800–12,800 and narrow molecular weight distributions (*M_w*/*M_n* ≤ 1.63).

Keywords: compressed CO₂; solventless reaction; epoxide; copolymerisation; polycarbonates; metalloporphyrin; chromium; fluorinated catalyst

1. Introduction

Carbon dioxide in compressed form is an attractive green alternative to organic solvents in synthetic chemistry due to its intrinsic low toxicity and availability. Particularly, the coupling of carbon dioxide (CO₂) with epoxides [1–5] is a topic of great interest due to the economic and environmental benefits arising from the utilisation of renewable sources for the preparation of polycarbonates or cyclic carbonates [6–9], and the growing concern on the greenhouse effect [10–15]. There is substantial literature on catalyst development for CO₂ insertions into epoxides, most of which consist of transition-metal complexes modified with N-donor ligands [16–27]. However, the low polarity of CO₂ often generates insolubility problems when transition-metal complexes are employed as catalysts. To address this issue, the introduction of fluorinated groups in the ligands is, in general, a promising strategy to improve the solubility of organometallic catalysts in compressed CO₂ [28].

In this context, metalloporphyrins are particularly attractive among the homogeneous catalysts, since their aromatic heterocycle can be easily modulated by the introduction of several peripheral substituents that may increase their solubility in compressed CO₂, and also because they are able to coordinate with a wide range of different transition metals, thus offering the possibility of fine-tuning the catalytic activity and selectivity [29–36].

Recently, we reported the application of *meso*-phenyl Mn(III) porphyrins as highly efficient catalysts for coupling the reactions of epoxides with CO₂, showing that the introduction of electron withdrawing halogen atoms in the *ortho* positions of *meso*-tetraphenylporphyrin manganese(III) complexes strengthens the Lewis acidity of the metal centre, thereby increasing their catalytic activity [37]. Earlier, in 2000, Holmes reported the use of tetrakis(pentafluorophenyl)porphyrinato chromium(III) chloride (6) in the copolymerisation reaction of cyclohexene oxide with CO₂ under supercritical conditions [20]. However, these catalysts originated polycarbonates with a low number-average molecular weight ($M_n \approx 3500$). In addition, the preparation of such a catalyst involves the use of an expensive perfluorinated reagent and low synthetic yield is obtained, resulting from its laborious purification procedure. So, we hypothesised that a convenient alternative could be achieved by the introduction of trifluoromethyl groups in the *meso*-aryl porphyrin's backbone. Such electron withdrawing groups would not only promote the catalyst's solubility in compressed CO₂, but could also increase the Lewis acidity of the metal centre and consequently improve its catalytic properties for CO₂/epoxide couplings.

In this paper, we present the catalytic evaluation of metal complexes of *meso*-arylporphyrins (Cr(III), Fe(III), and Zn(II)) in the coupling reaction of epoxides with compressed CO₂, in the absence of added solvent. For the Cr(III) catalysts, the effect of the fluorine atoms on the *meso*-aryl porphyrins are appraised regarding catalytic activity and selectivity for the alternating copolymerisation of cyclohexene oxide and CO₂. We further describe the synthesis of the fluorinated Cr(III)-porphyrin catalyst, tetrakis(4-trifluoromethylphenyl)porphyrinatochromium(III) chloride (7), whose potentialities are explored in this reaction.

2. Results and Discussion

2.1. Synthesis of the Catalysts

The preparation of metalloporphyrin complexes 1–6 (Figure 1) was accomplished based on recently developed methods by Coimbra's group [38,39] through the condensation of pyrrole with the desired aldehydes, followed by metal insertion through the reaction of free-base porphyrins with the appropriate metal salts [40,41].

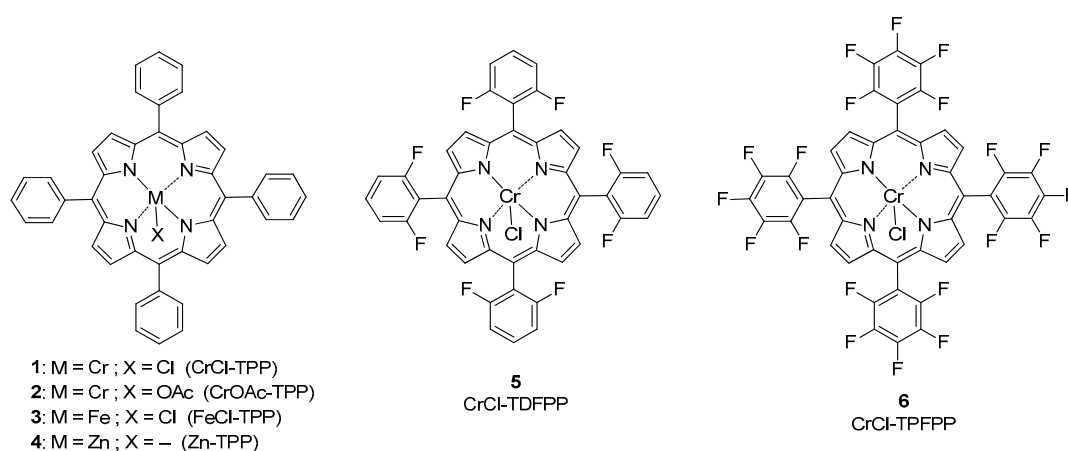
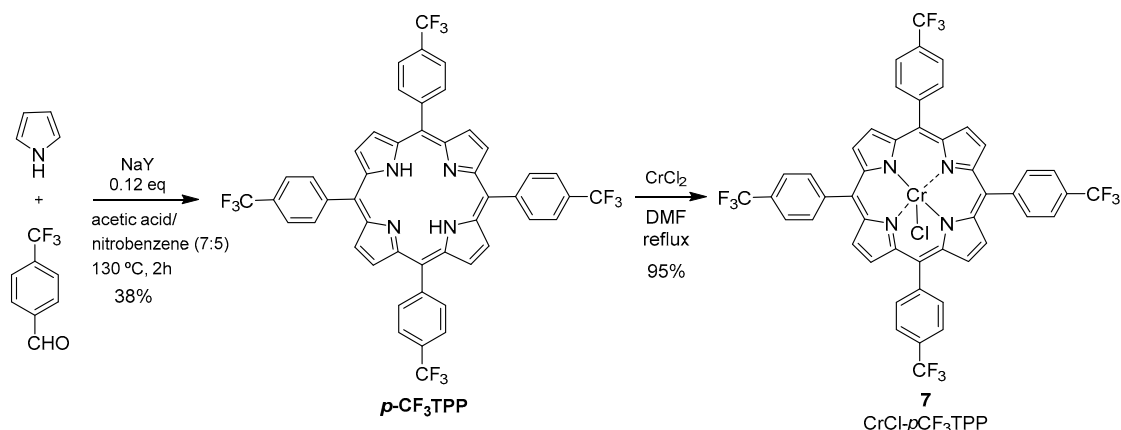


Figure 1. Metalloporphyrin catalysts. M, metal; X, co-axial ligand.

The metalloporphyrin **7**, previously reported in [42–45] was synthesised, in high yields, by the reaction of equimolar amounts of pyrrole with 4-(trifluoromethyl)benzaldehyde in a nitrobenzene/acetic acid mixture, using NaY zeolite as solid catalyst [39], followed by the complexation of *p*-CF₃TPP with CrCl₂ and in situ air oxidation [40] in refluxing DMF (Scheme 1).



2.2. Coupling Reactions of Cyclohexene Oxide with CO₂

2.2.1. Effect of the Metal

The effects of the metal (M) and co-axial ligand (X) on the catalytic activity and selectivity in the coupling reaction of cyclohexene oxide (CHO) and CO₂ using tetraphenylporphyrin (TPP) as a model N-donor ligand (Figure 1) were first appraised. The reactions were performed in the absence of solvent, under previously optimised conditions (50 bar CO₂, 80 °C), using a 0.07 mol % catalyst [37], with and without bis(triphenylphosphine)iminium chloride (PPNCl) as a co-catalyst. The results are presented in Table 1.

Table 1. Metal effect on the selectivity of coupling reactions of CO₂ with cyclohexene oxide. ^a

Entry	Catalyst	Co-cat	Conversion ^b (%)	TON ^c	Selectivity ^d	
					PCHC (%)	CHC (%)
1	1 (CrCl-TPP)	-	0	0	-	-
2	1 (CrCl-TPP)	PPNCl	79	1128	98	2
3	2 (CrOAc-TPP)	PPNCl	74	1056	92	8
4	3 (FeCl-TPP)	-	0	0	-	-
5	3 (FeCl-TPP)	PPNCl	14	192	0	100
6	4 (Zn-TPP)	-	0	0	-	-
7	4 (Zn-TPP)	PPNCl	34	480	0	100

^a Reaction conditions: CHO (39.5 mmol, 4 mL); catalyst: 0.07 mol %; co-catalyst (when indicated): PPNCl 0.07 mol %; T = 80 °C; P(CO₂) = 50 bar; t = 24 h. ^b Conversion determined by ¹H NMR. ^c turnover number calculated as mol_(converted substrate)/mol_(catalyst). ^d Selectivity determined by ¹H NMR, through integral ratio of polycarbonate/cyclic carbonate.

Under these conditions, all of the TPP-based metalloporphyrin catalysts required the use of a co-catalyst to promote the coupling reaction of CHO with CO₂. Among them, Cr(III) catalytic

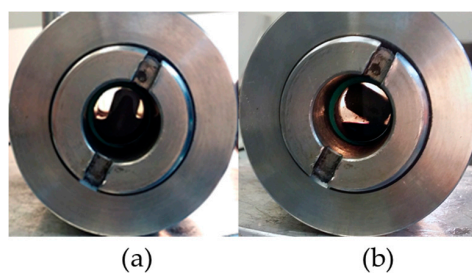


Figure 2. (a) Homogeneous phase at beginning of reaction; (b) polymer precipitation after a 2 h reaction (Reaction conditions: P_{CO_2} = 50 bar; T = 80 °C; 39.5 mmol CHO; 0.07% catalyst 7; 0.07% PPNCI).

Table 3. Effects of temperature (T) and pressure (P) in CO_2 /cyclohexene oxide copolymerisation using catalyst 7. ^a

CHO + CO₂ $\xrightarrow[\text{PPNCI}]{\text{Catalyst 7}}$ PCHC

Entry	T (°C)	P_{CO_2} (bar)	Conv. ^b (%)	TON ^c	Polymers (%)	Isolated Yield (%) ^d	% CO ₂ ^e	$M_n \cdot 10^{-3}$ ^f	M_w/M_n ^f
1	50	50	77	1080	99	30	98	6.8	1.43
2	80	50	86	1224	99	58	98	4.8	1.25
3	80	10	70	1008	99	42	99	9.1	1.45
4	80	70	86	1224	96	60	98	12.5	1.38
5	80	110	84	1176	98	65	98	7.8	1.37
6	80	150	65	936	97	47	98	5.0	1.63

^a Reaction conditions: CHO (39.5 mmol, 4 mL); catalyst 7: 0.07 mol %; co-catalyst: PPNCI 0.07 mol %; t = 24 h. ^b % Conversion determined by ¹H NMR. ^c turnover number calculated as $\text{mol}_{(\text{converted substrate})} / \text{mol}_{(\text{catalyst})}$. ^d Isolated yield for poly(cyclohexane)carbonate, based on weighted mass of obtained product, relatively to weighted mass of epoxide and CO₂. ^e % CO₂ content in polymers determined by ¹H NMR integral ratio of carbonate linkages/(carbonate linkages+ether linkages). ^f Number average molecular weight and polydispersity determined by GPC, using polystyrene as standard.

At a lower temperature (50 °C), the reaction proceeded with a slightly lower conversion (77%) than that obtained at 80 °C, but the selectivity for copolymers and the carbonate content was similar (Table 3, entries 1 and 2). This observation differs from the results obtained with a CrCl-TPFPP/DMAP catalytic system under supercritical conditions [20], where the outcome of the reaction was strongly temperature-dependent, with only oligomeric polyether formation being observed at lower temperatures (70 °C), while higher reaction temperatures (95–110 °C) were found, in general, to lead to higher CO₂ incorporations and higher polymer yields. With the reaction temperature set on 80 °C, the effect of CO₂ pressure was then evaluated in the range of 10–150 bar (Table 3, entries 2–6). We observed that, at 10 bar CO₂, a conversion of 70% is achieved, with almost full selectivity for polymers, containing 99% of carbonate content (Table 3, entry 3). This result seems also to contrast with the results obtained with a CrCl-TPFPP/DMAP catalytic system, for which a low-pressure CO₂ atmosphere resulted in only oligomeric products ($M_n \sim 600 \text{ g} \cdot \text{mol}^{-1}$) obtained in poor yields and with low CO₂ incorporation [20]. In the range of 50–110 bar CO₂, conversions are considerably higher (84–86%) than at 10 bar, with no significant effects being observed in this pressure range, either in catalytic activity (TON's = 1008–1224) or selectivity for copolymers (96–99%) (Table 3, entries 2–5). However, a further increase of CO₂ pressure to 150 bar led to a significant decrease in polymer yield, resulting from lower catalytic activity (Table 3, entry 6). This outcome can be directly observed from Figure 3, which illustrates the influence of CO₂ pressure in the isolated yields of the copolymer PCHC, showing a maximum value at 110 bar CO₂, and a visible drop at 150 bar CO₂.

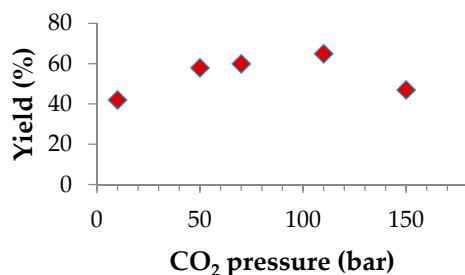


Figure 3. Effect of CO₂ pressure in isolated yields of the copolymer PCHC.

This effect is probably due to the phase behaviour, since the increase of CO₂ pressure leads to variations in both the density of the reaction mixture and the molar ratio of CHO to CO₂. Therefore, the decrease in yield and molecular weight when the reaction is carried out at 150 bar CO₂ pressure might be attributed to a reduction in effective CHO concentration, which occurs when the phase boundary for the system is crossed, in agreement with previous studies [20,46]. Moreover, a notable effect of CO₂ pressure was observed in the molecular weight of the polymers, with the highest number-average molecular weight (in the range of 12,500 g·mol⁻¹) being obtained when the reaction is performed at a CO₂ pressure of 70 bar (Table 3, entry 4), while the lowest polydispersity value ($M_w/M_n = 1.25$) is obtained when the reaction is carried out at a 50 bar CO₂ pressure (Table 3, entry 2). In this case, the molecular weight of the polymer obtained showed a monomodal distribution, while in the rest of the other experiments bimodal distributions were obtained (see discussion in Section 2.2.4).

2.2.4. Characterisation of PCHC Copolymers

The reaction's crude was dried in vacuum at 100 °C for 5 h, to eliminate unreacted CHO. After washing with *n*-hexane to remove possible traces of CHC, the residue was filtered and dried under vacuum at 100 °C for 12 h. Finally, the purified copolymer was characterised by ¹H and ¹³C NMR spectroscopy and gel permeation chromatography (GPC).

The ¹H NMR spectrum of PCHC (Figure 4) shows a signal at $\delta = 4.64$ ppm, typical of the methine proton (H₁ in PCHC) of the repeating oxycarbonyloxy unit, while a very narrow singlet at $\delta = 3.57$ ppm corresponding to oxy units was scarcely perceptible, which confirmed that the polymers were comprised mostly of carbonate content (98%) and contained a diminutive percentage of ether linkages.

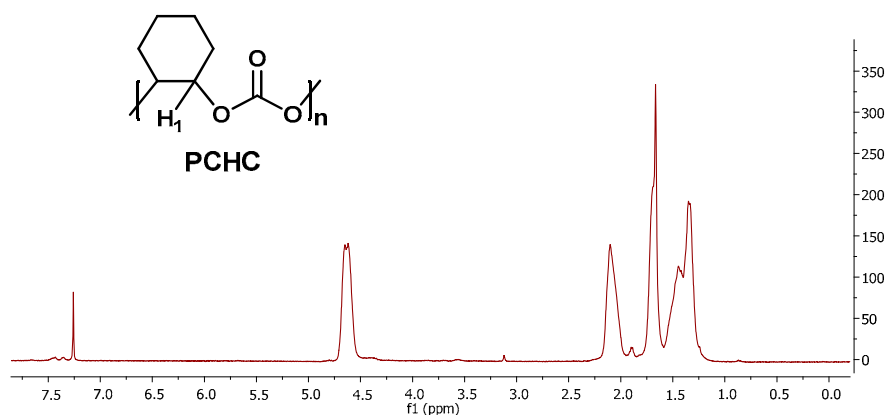


Figure 4. ¹H NMR spectrum of PCHC in CDCl₃ at 25 °C (reaction conditions of Table 3, entry 2).

The ¹³C NMR spectrum (Figure 5), performed in CDCl₃, presents a dominant C=O signal at $\delta = 153.9$ ppm, which has previously been assigned to the carbonate carbon atom of *m*-centred structural units ((*mmm*), (*mnr*), (*rmr*)), while minor resonances at $\delta = 153.2$ and 153.4 ppm can

be assigned to r-centered units ((rrr), (rrm), (mrm)) [47–49], suggesting that the ring-opening copolymerisation mechanism occurs without a defined stereocontrol.

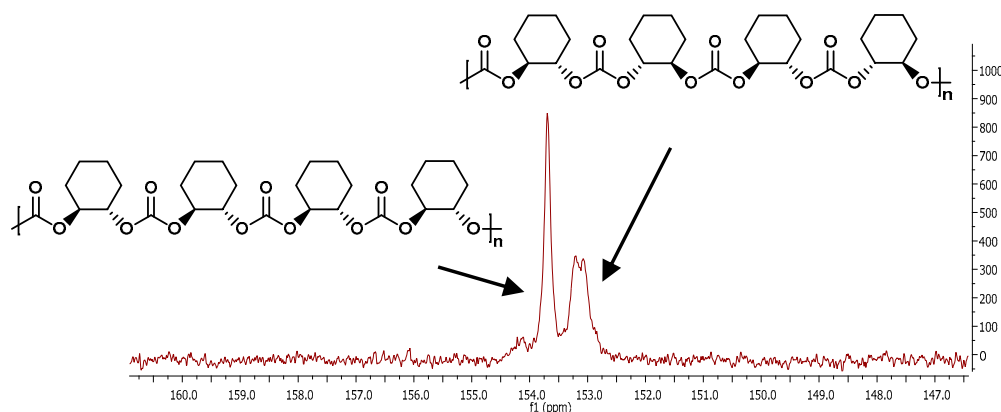


Figure 5. Carbonate region of ^{13}C NMR spectrum of PCHC in CDCl_3 at $25\text{ }^\circ\text{C}$ (reaction conditions of Table 3, entry 2).

GPC analysis, performed in toluene, and calibrated against a polystyrene standard, allowed the calculation of the number-average molecular weights (M_n) of the copolymers, which were in the range of $4800\text{--}12,500\text{ g}\cdot\text{mol}^{-1}$. Furthermore, the molecular weight distributions (M_w/M_n) were determined to be in the range $1.25\text{--}1.63$, which represent significant progress over distributions previously reported for some scCO_2 -based systems [20,50]. GPC chromatograms of the copolymers (Figure 6) showed elution curves with unimodal (in the case of entry 2, Table 3) or bimodal distributions (entries 1, 3–6, Table 3), which are indicative of a chain transfer process or a different chain termination step.

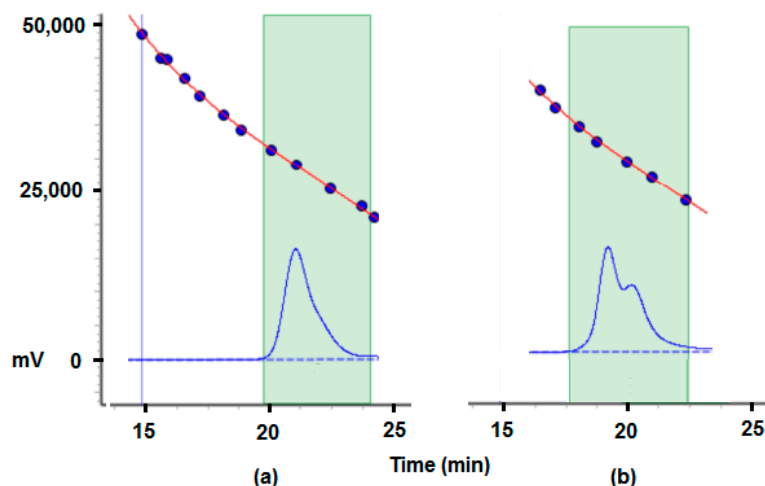


Figure 6. GPC chromatograms of PCHC in toluene, using a polystyrene standard, obtained under the reaction conditions of: (a) $P_{\text{CO}_2} = 50\text{ bar}$, $T = 80\text{ }^\circ\text{C}$ (entry 2, Table 3); (b) $P_{\text{CO}_2} = 70\text{ bar}$, $T = 80\text{ }^\circ\text{C}$ (entry 4, Table 3).

2.2.5. MALDI-TOF Analysis and Mechanistic Considerations

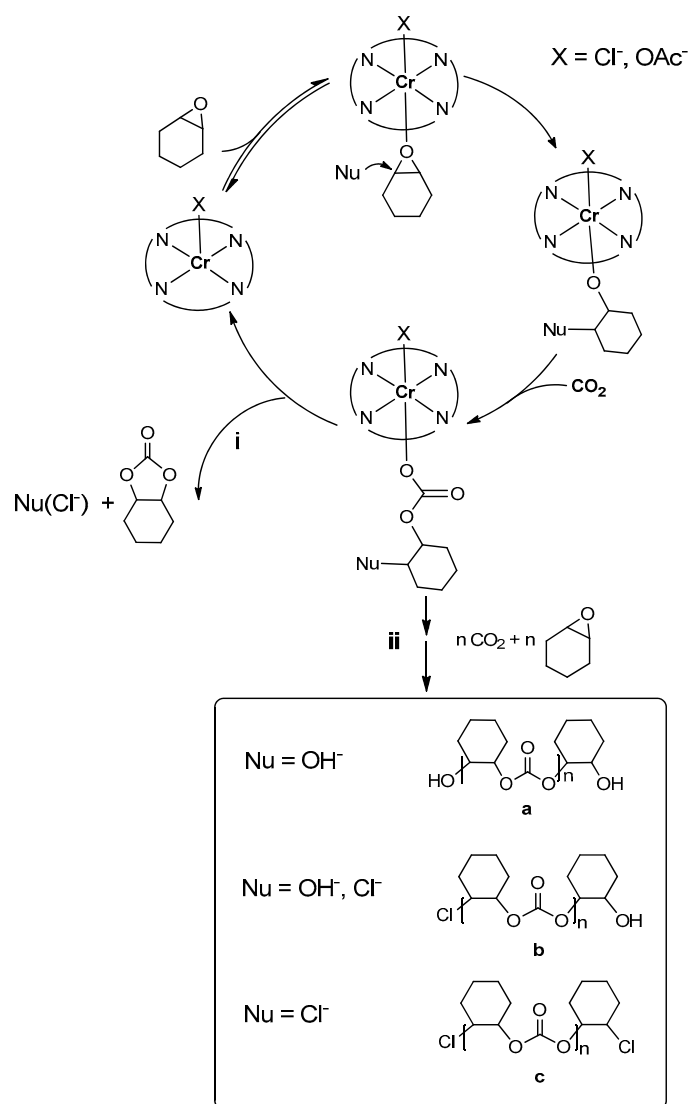
The matrix assisted laser desorption ionization time-of-flight mass spectrometry (MALDI-TOF) mass spectra of the polymers resulting was performed in order to analyse the chain end groups of the polycarbonates and draw conclusions about the probable reaction mechanism.

The MALDI-TOF mass spectra of the polymers obtained present repeating units of $142\text{ }m/z$ corresponding to a cyclohexylcarbonate $-\text{C}_6\text{H}_{10}\text{C}(\text{O})\text{O}-$ fragment (Figures S1–S6, Supplementary

Information). In the case of the polymer obtained from entry 2 in Table 3, the main distribution presented peaks at m/z 5981.6, 6124.1, and 6266.0 (Figure S2) that correspond to chains containing two -OH terminal groups (**a** + K in Scheme 2, expected for $n = 41\text{--}43$ $\text{HO}(\text{C}_7\text{H}_{10}\text{O}_3)_n\text{C}_6\text{H}_{10}\text{OH}$ m/z 5981.1, 6123.2, 6265.3). This suggests that the initiation step involves the epoxide opening by a nucleophilic attack, with -OH arising from water traces present in the reactor, and water is also involved in the final step to form a -OH chain end (Scheme 2).

Minor peaks distributions fitted with the presence of Cl^- as end group as well as -OH (**b**, Scheme 2, observed m/z 5963.79, 6105.63 (Figure S2); expected for $n = 41, 42$; m/z 5960.6, 6102.7). In this case the presence of a main chain corresponded with the observation of a single band in the GPC analysis and low M_w/M_n polydispersity.

In the experiments run at different pressure and temperature (entries 1,3–6, Table 3), which presented bimodal distribution in the GPC analysis, the MALDI-TOF mass spectra showed mixtures of three species (Figures S1, S3–S6, Supplementary Materials). The results indicated that chains **a** and **b** were present (Scheme 2), and the third peak distribution with peaks observed at m/z 6000.91 and 6141.42 may correspond to polymers with two -Cl final groups (**c** + Na, Scheme 2, expected for $n = 41, 42$; m/z 6000.9, 6141.4).



Scheme 2. Proposed mechanism for the polymerization of CHO with CO_2 using 7/PPNCr catalytic system.

Consequently, the mechanism may involve the opening of the epoxide, presumably after coordinating to the metal center, by the Cl^- from PPNCI or OH^- from water. The alkoxo species thus formed inserts CO_2 and produces the cyclic carbonate by intramolecular attack, generating the nucleophile that, in this case, may be Cl^- since OH^- is not a good leaving group (i, in Scheme 2). An alternate insertion of epoxide and CO_2 leads to the polycarbonate growing chain (ii, in Scheme 2). As evidenced by the chain end group analysis, termination may occur by different pathways, including by the combination of two growing chains or by the hydrolysis of water. The polymer obtained under optimal reaction conditions (80 °C and 50 bar CO_2) shows a monomodal distribution, which suggests that the chain transfer, responsible for different length polymers, is probably a minor process. Instead, using higher CO_2 pressures, precipitation of the polymer in the compressed CO_2 medium may generate the formation of different chains' length, which explains the bimodal molecular weight distributions. At lower CO_2 pressure (10 bar) or temperature (50 °C), the lower conversions obtained may induce a similar effect.

3. Materials and Methods

3.1. Reagents

Cyclohexene oxide was purchased from Sigma-Aldrich, dried over alumina and stored under inert atmosphere. Carbon dioxide (SCF Grade, 99.9993%, Abelló Linde, Barcelona, Spain) was previously passed by an Agilent oxygen/moisture trap. The rest of reagents and solvents were purchased from Sigma-Aldrich (Madrid, Spain) unless otherwise stated.

3.2. Equipment

The ^1H NMR and ^{13}C NMR spectra were recorded in a 400 MHz Mercury instrument (VARIAN, Palo Alto, CA, USA), in CDCl_3 using tetramethylsilane as internal standard. Gel permeation chromatography (GPC) measurements (URV, Tarragona, Spain) were made in toluene, versus polystyrene standards, on a Millipore-Waters 510 HPLC Pump device (Milford, MA, USA) using a three-serial column system (MZ-Gel 100 Å, MZ-Gel 1000 Å, MZ-Gel 10,000 Å linear columns, Millipore-Waters, Milford, MA, USA) with UV-Detector (ERC-7215) and IR-Detector (ERC-7515a, Millipore-Waters, Milford, MA, USA). The software used to get the data was NTeqGPC 5.1 (Millipore-Waters, Milford, MA, USA). Samples were prepared as follows: 5 mg of the copolymer was dissolved with 2 mL of toluene (HPLC grade). MALDI-TOF analyses were performed on a Voyager System 4412 instrument equipped with a 337 nm nitrogen laser (Applied Biosystems, Foster City, CA, USA). All spectra were acquired in the positive ion reflector mode. Dithranol (Sigma-Aldrich, Madrid, Spain) was used as matrix, which was dissolved in MeOH (Panreac, Barcelona, Spain) at a concentration of $10 \text{ mg}\cdot\text{mL}^{-1}$. The polymer (5 mg) was dissolved in 1 mL of CHCl_3 (Euriso-Top, Saint-Aubin, France). One microliter (1 μL) of the sample, 1 μL of the matrix, and 1 μL of potassium trifluoroacetate (KTFA) solution in the case of polymers (1 mg of KTFA in 1 mL of THF) were deposited consecutively on the stainless steel sample holder and allowed to dry before introduction into the mass spectrometer. Three independent measurements were made for each sample. For each spectrum, 100 laser shots were accumulated. Elemental analysis were done at the Serveis Tècnics de Recerca (Universitat de Girona, Spain).

3.3. Preparation of Metalloporphyrin Catalysts

The porphyrins 5,10,15,20-tetraphenylporphyrin (TPP), 5,10,15,20-tetra(2,6-difluorophenyl)porphyrin (TDFPP), 5,10,15,20-tetra(2,3,4,5,6-pentafluorophenyl)porphyrin (TPFPP), and 5,10,15,20-tetra(4-trifluoromethylphenyl)porphyrin (*p*- CF_3 TPP) were prepared by reacting pyrrole with the corresponding aldehydes in equimolar amounts, in a nitrobenzene/acetic acid mixture, according to previously reported methods [38,39,51,52]. Then, the resulting free-base porphyrins were reacted with the desired metal salt to achieve the corresponding metalloporphyrin catalysts 1–7 [53].

Synthesis of 5,10,15,20-tetrakis(4-trifluoromethylphenyl)porphyrinatochromium(III) Chloride (7)

The free base porphyrin *p*-CF₃TPP [51] (0.400 g, 0.45 mmol) was dissolved in 15 mL of dimethylformamide (DMF). The mixture was stirred under reflux at 170 °C. After approximately 10 min, CrCl₂ (0.095 g, 0.77 mmol) was added to the refluxing solution. After 30 min, an aliquot was taken from the mixture and analysed by UV-VIS spectroscopy, which indicated that free *p*-CF₃TPP still remained in solution. So, a further amount of CrCl₂ (0.073 g, 0.59 mmol) was added to the solution, refluxing for another 20 min, until no free *p*-CF₃TPP was found by UV-VIS. At the end, the reaction mixture was allowed to cool to room temperature and poured into 400 mL of ice-cold water. After the solid was filtered out and washed three times with water, it was dried under vacuum at 100 °C. The crude product was purified by column chromatography over alumina with CHCl₃ as the eluent. After solvent evaporation, the product was dried overnight under vacuum at 100 °C, yielding the chromium porphyrin complex CrCl-*p*-CF₃TPP (7) as a dark green solid, in 95% yield (0.415 g, 0.43 mmol). UV-VIS (CH₂Cl₂): λ_{max}/nm (ε/dm³·mol⁻¹·cm⁻¹): 446 (130,930), 563 (8473), 601 (5857). MS (ESI): *m/z* for C₄₈H₂₄F₁₂N₄CrCl [M + 2Na]⁺ 1018.1738. Elemental analysis (%) calculated for C₄₈H₂₄F₁₂N₄CrCl·CHCl₃·H₂O: C 53.0, H 2.5, N 5.1; found: C 50.2, H 2.4, N 5.2.

3.4. Synthesis and Characterisation of Copolymers

3.4.1. General Procedure of Catalytic Reactions of Epoxides with CO₂

The reactions were carried out in a 100 mL Berghof stainless steel autoclave (Berghof, Eningen, Germany). The catalyst (0.07%) and co-catalyst (0.07%) (when indicated) were placed inside the autoclave and kept for 3 h, under vacuum, at 80 °C. Then, the epoxide substrate (4 mL), previously dried over alumina, was injected into the autoclave via cannula. The autoclave was then pressurized with CO₂, and the reaction proceeded at the desired temperature. At the end of the reaction, the autoclave was cooled and slowly depressurized. The % of conversion was determined by ¹H NMR of the crude mixture, using mesitylene as standard. Selectivity was calculated by integral ratio between polycarbonate and cyclic carbonate. The work-up was performed only when polymeric products were obtained, and is described below.

3.4.2. Poly(cyclohexenecarbonate) (PCHC)

The crude mixture was evaporated and the residue was dried in vacuum at 100 °C for 5 h. The solid residue was then washed three times with *n*-hexane, filtered, and dried under vacuum at 100 °C overnight. The resulting polymer was dissolved in CDCl₃ and analyzed by NMR spectroscopy. The polymer yield was calculated from the mass of the isolated product relative to the weighted mass of epoxide and the CO₂ weight of the catalyst and co-catalyst [54]. The % of CO₂ content was calculated from ¹H NMR data by the integral ratio between copolymer carbonate linkages (δ = 4.64 ppm) with respect to the ether linkage signals (δ = 3.57 ppm). Typical data: ¹H NMR (400 MHz, CDCl₃): δ/ppm 4.64 (br s, 2H, CHOC(O)O), 2.20–1.95, 1.76–1.60 (br s, 4H, -CH₂-), 1.55–1.25 (br m, 4H, -CH₂-). ¹³C NMR (100 MHz, CDCl₃): δ/ppm 153.9, 153.2 (-C(O)), 29.7, 29.4, 28.9 (-CH₂), 23.1, 22., 22.3 (-CH₂).

4. Conclusions

Metal complexes of *meso*-arylporphyrins (Cr(III), Zn(II), and Fe(III)) have efficiently catalysed the coupling reaction between CO₂ and cyclohexene oxide, with Cr(III)porphyrin 7/PPNCl being the most active and selective for the formation of copolymers. This trifluoromethyl-based catalytic system is an attractive alternative to other fluorinated catalysts, considering its easy synthesis, high selectivity for copolymerisation, and high solubility in the substrate and compressed carbon dioxide medium, avoiding the use of any additional harmful solvent. Using this new catalytic system, the CO₂ pressure was found to affect the outcome of the reaction, with the best copolymer yield being obtained at 110 bar CO₂, the higher number-average molecular weight (12,500 g·mol⁻¹) being obtained at a CO₂ pressure of 70 bar, and the lowest polydispersity value (1.25) at 50 bar CO₂ pressure. The formed copolymers

have shown narrow molecular weight distributions ($M_w/M_n \approx 1.2$ – 1.6), and high carbonate contents (up to 98% CO₂ incorporation), when compared with other Cr(III)-porphyrin based catalytic systems.

Supplementary Materials: The following are available online at www.mdpi.com/2073-4344/7/7/210/s1, Figure S1. MALDI TOF spectra of PCHC obtained under the reaction conditions of P_{CO2} = 50 bar, T = 50 °C (entry 1, Table 3), Figure S2. MALDI TOF spectra of PCHC obtained under the reaction conditions of P_{CO2} = 10 bar, T = 80 °C (entry 3, Table 3), Figure S3. MALDI TOF spectra of PCHC obtained under the reaction conditions of P_{CO2} = 110 bar, T = 80 °C (entry 5, Table 3), Figure S4. MALDI TOF spectra of PCHC obtained under the reaction conditions of P_{CO2} = 150 bar, T = 80 °C (entry 6, Table 3), Figure S5. MALDI TOF spectra of PCHC obtained under the reaction conditions of P_{CO2} = 110 bar, T = 80 °C (entry 5, Table 3), Figure S6. MALDI TOF spectra of PCHC obtained under the reaction conditions of P_{CO2} = 150 bar, T = 80 °C (entry 6, Table 3).

Acknowledgments: The authors are thankful to Ministerio de Economía y Competitividad (CTQ2016-75016-R), Departament d'Economia i Coneixement (2014 SGR 670), and to Fundação para a Ciência e a Tecnologia (FCT) for the financial support to Coimbra Chemistry Centre (PEst-OE/QUI/UI0313/2014). RMBC thanks FCT for post-doc grant SFRH/BPD/100537/2014. LDD thanks CNPq for PhD grant 232620/2014-8/GDE.

Author Contributions: R.M.B.C, M.M.P, and A.M.M.-B. conceived and designed the experiments; R.M.B.C. and L.D.D. performed the experiments; R.M.B.C., L.D.D., M.M.P., and C.C. analysed the data; M.M.P., A.M.M.-B., C.C., and R.R. contributed reagents/materials/analysis tools; and R.M.B.C., M.M.P., and A.M.M.-B wrote the paper.

Conflicts of Interest: The authors declare no conflict of interest.

References

1. Whiteoak, C.J.; Kleij, A.W. Catalyst development in the context of ring expansion-addition of carbon dioxide to epoxides to give organic carbonates. *Synlett* **2013**, *24*, 1748–1756. [[CrossRef](#)]
2. Sakakura, T.; Kohno, K. The synthesis of organic carbonates from carbon dioxide. *Chem. Commun.* **2009**, *21*, 1312–1330. [[CrossRef](#)] [[PubMed](#)]
3. Dai, W.-L.; Luo, S.-L.; Yin, S.-F.; Au, C.-T. The direct transformation of carbon dioxide to organic carbonates over heterogeneous catalysts. *Appl. Catal. A Gen.* **2009**, *366*, 2–12. [[CrossRef](#)]
4. Lu, X.-B.; Darensbourg, D.J. Cobalt catalysts for the coupling of CO₂ and epoxides to provide polycarbonates and cyclic carbonates. *Chem. Soc. Rev.* **2012**, *41*, 1462–1484. [[CrossRef](#)] [[PubMed](#)]
5. Kember, M.R.; Buchard, A.; Williams, C.K. Catalysts for CO₂/epoxide copolymerization. *Chem. Commun.* **2011**, *47*, 141–163. [[CrossRef](#)] [[PubMed](#)]
6. Coates, G.W.; Moore, D.R. Discrete metal-based catalysts for the copolymerization of CO₂ and epoxides: Discovery, reactivity, optimization and mechanism. *Angew. Chem. Int. Ed.* **2004**, *43*, 6618–6639. [[CrossRef](#)] [[PubMed](#)]
7. Clemens, J.H. Reactive applications of cyclic alkylene carbonates. *Ind. Eng. Chem. Res.* **2003**, *42*, 663–674. [[CrossRef](#)]
8. Martin, C.; Fiorani, G.; Kleij, A.W. Recent advances in the catalytic preparation of cyclic organic carbonates. *ACS Catal.* **2015**, *5*, 1353–1370. [[CrossRef](#)]
9. North, M.; Pasquale, R.; Young, C. Synthesis of cyclic carbonates from epoxides and CO₂. *Green Chem.* **2010**, *12*, 1514–1539. [[CrossRef](#)]
10. Sakakura, T.; Choi, J.-C.; Yasuda, H. Transformation of carbon dioxide. *Chem. Rev.* **2007**, *107*, 2365–2387. [[CrossRef](#)] [[PubMed](#)]
11. Liu, V.; Wu, V.; Jackstell, R.; Beller, M. Using carbon dioxide as a building block in organic synthesis. *Nat. Commun.* **2015**, *6*, 5933–5948. [[CrossRef](#)] [[PubMed](#)]
12. Omae, I. Recent developments in carbon dioxide utilization for the production of organic chemicals. *Coord. Chem. Rev.* **2012**, *256*, 1384–1405. [[CrossRef](#)]
13. Ma, J.; Sun, N.; Zhang, X.; Zhao, N.; Xiao, F.; Wei, W.; Sun, Y. A short review of catalysis for CO₂ conversion. *Catal. Today* **2009**, *148*, 221–231. [[CrossRef](#)]
14. Razali, N.A.M.; Lee, K.T.; Bhatia, S.; Mohamed, A.R. Heterogeneous catalysts for production of chemicals using carbon dioxide as raw material: A review. *Energy Rev.* **2012**, *16*, 4951–4964. [[CrossRef](#)]
15. Darensbourg, D.J.; Holtcamp, M.W. Catalysts for the reaction of epoxides and carbon dioxide. *Coord. Chem. Rev.* **1996**, *153*, 155–174. [[CrossRef](#)]
16. North, M. Synthesis of cyclic carbonates from epoxides and carbon dioxide using bimetallic aluminium(salen) complexes. *ARKIVOC* **2012**, *2012*, 610–628.

17. Clegg, W.; Harrington, R.W.; North, M.; Pasquale, R. Cyclic carbonate synthesis catalysed by bimetallic aluminium-salen complexes. *Chem. Eur. J.* **2010**, *16*, 6828–6843. [[CrossRef](#)] [[PubMed](#)]
18. Harrold, N.D.; Li, Y.; Chisholm, M.H. Studies of ring-opening reactions of styrene oxide by chromium tetraphenylporphyrin initiators. Mechanistic and stereochemical considerations. *Macromolecules* **2013**, *46*, 692–698. [[CrossRef](#)]
19. Ohkawara, T.; Suzuki, K.; Nakano, K.; Mori, S.; Nozaki, K. Facile estimation of catalytic activity and selectivities in copolymerization of propylene oxide with carbon dioxide mediated by metal complexes with planar tetradentate ligand. *J. Am. Chem. Soc.* **2014**, *136*, 10728–10735. [[CrossRef](#)] [[PubMed](#)]
20. Mang, S.; Cooper, A.I.; Colclough, M.E.; Chauhan, N.; Holmes, A.B. Copolymerization of CO₂ and 1,2-cyclohexene oxide using a CO₂-soluble chromium porphyrin catalyst. *Macromolecules* **2000**, *33*, 303–308. [[CrossRef](#)]
21. Darensbourg, D.J.; Fitch, S.B. An Exploration of the coupling reactions of epoxides and carbon dioxide catalyzed by tetramethyltetraazaannulene chromium(III) derivatives: Formation of copolymers versus cyclic carbonates. *Inorg. Chem.* **2008**, *47*, 11868–11878. [[CrossRef](#)] [[PubMed](#)]
22. Dengler, J.E.; Lehenmeier, M.W.; Klaus, S.; Anderson, C.E.; Herdtweck, E.; Rieger, B. A one-component iron catalyst for cyclic propylene carbonate synthesis. *Eur. J. Inorg. Chem.* **2011**, *2011*, 336–343. [[CrossRef](#)]
23. Cuesta-Aluja, L.; Djoufak, M.; Aghmiz, A.; Rivas, R.; Christ, L.; Masdeu-Bultó, A.M. Novel chromium(III) complexes with N₄-donor ligands as catalysts for the coupling of CO₂ and epoxides in supercritical CO₂. *J. Mol. Catal. A Chem.* **2014**, *381*, 161–170. [[CrossRef](#)]
24. Adolph, M.; Zevaco, T.A.; Altesleben, C.; Walter, O.; Dinjus, E. New cobalt, iron and chromium catalysts based on easy-to-handle N₄-chelating ligands for the coupling reaction of epoxides with CO₂. *Dalton Trans.* **2014**, *43*, 3285–3296. [[CrossRef](#)] [[PubMed](#)]
25. Sheng, X.; Qiao, L.; Qin, Y.; Wang, X.; Wang, F. Highly efficient and quantitative synthesis of a cyclic carbonate by iron complex catalysts. *Polyhedron* **2014**, *74*, 129–133. [[CrossRef](#)]
26. Adolph, M.; Zevaco, T.A.; Altesleben, C.; Staudt, S.; Dinjus, E. New zinc catalysts based on easy-to-handle N₄-chelating ligands for the coupling reaction of epoxides with CO₂. *J. Mol. Catal. A Chem.* **2015**, *400*, 104–110. [[CrossRef](#)]
27. Mercadé, E.; Zangrando, E.; Claver, C.; Godard, C. Robust zinc complexes that contain pyrrolidine-based ligands as recyclable catalysts for the synthesis of cyclic carbonates from carbon dioxide and epoxides. *ChemCatChem* **2016**, *8*, 234–243. [[CrossRef](#)]
28. Campos-Carrasco, A.; Tortosa-Estorach, C.; Masdeu-Bultó, A.M. Rh(I) complexes with fluorinated 2,2'-bipyridines. *Inorg. Chem. Commun.* **2012**, *18*, 61–64. [[CrossRef](#)]
29. Stamp, L.M.; Mang, S.A.; Holmes, A.B.; Knights, K.A.; de Miguel, Y.R.; McConvey, I.F. Polymer supported chromium porphyrin as catalyst for polycarbonate formation in supercritical carbon dioxide. *Chem. Commun.* **2001**, 2502–2503. [[CrossRef](#)]
30. Chatterjee, C.; Chisholm, M.H.; El-Khaldy, A.; McIntosh, R.D.; Miller, J.T.; Wu, T. Influence of the metal (Al, Cr, and Co) and substituents of the porphyrin in controlling reactions involved in copolymerization of propylene oxide and carbon dioxide by porphyrin metal(III) complexes. 3. Cobalt chemistry. *Inorg. Chem.* **2013**, *52*, 4547–4553. [[CrossRef](#)] [[PubMed](#)]
31. Chatterjee, C.; Chisholm, M.H. Influence of the metal (Al, Cr, and Co) and the substituents of the porphyrin in controlling the reactions involved in the copolymerization of propylene oxide and carbon dioxide by porphyrin metal(III) complexes. 2. Chromium chemistry. *Inorg. Chem.* **2012**, *51*, 12041–12052. [[CrossRef](#)] [[PubMed](#)]
32. Chatterjee, C.; Chisholm, M.H. The influence of the metal (Al, Cr, and Co) and the substituents of the porphyrin in controlling the reactions involved in the copolymerization of propylene oxide and carbon dioxide by porphyrin metal(III) complexes. 1. Aluminum chemistry. *Inorg. Chem.* **2011**, *50*, 4481–4492. [[CrossRef](#)] [[PubMed](#)]
33. Bai, D.; Duan, S.; Hai, L.; Jing, H. Carbon dioxide fixation by cycloaddition with epoxides, catalyzed by biomimetic metalloporphyrins. *ChemCatChem* **2012**, *4*, 1752–1758. [[CrossRef](#)]
34. Bai, D.; Wang, Q.; Song, Y.; Li, B.; Jing, H. Synthesis of cyclic carbonate from epoxide and CO₂ catalyzed by magnetic nanoparticle-supported porphyrin. *Catal. Commun.* **2011**, *12*, 684–688. [[CrossRef](#)]
35. Ema, T.; Miyazaki, Y.; Koyama, S.; Yano, Y.; Sakai, T. A bifunctional catalyst for carbon dioxide fixation: cooperative double activation of epoxides for the synthesis of cyclic carbonates. *Chem. Commun.* **2012**, *48*, 4489–4491. [[CrossRef](#)] [[PubMed](#)]

36. Ema, T.; Miyazaki, Y.; Taniguchi, T.; Takada, J. Robust porphyrin catalysts immobilized on biogenous iron oxide for the repetitive conversions of epoxides and CO₂ into cyclic carbonates. *Green Chem.* **2013**, *15*, 2485–2492. [[CrossRef](#)]
37. Cuesta-Aluja, L.; Castilla, J.; Masdeu-Bultó, A.M.; Henriques, C.A.; Calvete, M.J.F.; Pereira, M.M. Halogenated meso-phenyl Mn(III) porphyrins as highly efficient catalysts for the synthesis of polycarbonates and cyclic carbonates using carbon dioxide and epoxides. *J. Mol. Catal. A Chem.* **2016**, *423*, 489–494. [[CrossRef](#)]
38. Johnstone, R.A.W.; Nunes, M.L.P.J.; Pereira, M.M.; Gonsalves, A.M.A.R.; Serra, A.C. Improved Syntheses of 5,10,15,20-Tetrakisaryl- and Tetrakisalkylporphyrins. *Heterocycles* **1996**, *43*, 1423–1437. [[CrossRef](#)]
39. Silva, M.; Fernandes, A.; Bebian, S.S.; Calvete, M.J.F.; Ribeiro, M.F.; Burrows, H.D.; Pereira, M.M. Size and ability do matter! Influence of acidity and pore size on the synthesis of hindered halogenated meso-phenyl porphyrins catalysed by porous solid oxides. *Chem. Commun.* **2014**, *50*, 6571–6573. [[CrossRef](#)] [[PubMed](#)]
40. Chen, P.; Chisholm, M.H.; Gallucci, J.C.; Zhang, X.; Zhou, Z. Binding of propylene oxide to porphyrin- and salen-M(III) cations, where M = Al, Ga, Cr, and Co. *Inorg. Chem.* **2005**, *44*, 2588–2595. [[CrossRef](#)] [[PubMed](#)]
41. Azenha, E.G.; Serra, A.C.; Pineiro, M.; Pereira, M.M.; Melo, J.S.; Arnaut, L.G.; Formosinho, S.J.; Gonsalves, A.M.A.R. heavy-atom effects on metalloporphyrins and polyhalogenated porphyrins. *Chem. Phys.* **2002**, *280*, 177–190. [[CrossRef](#)]
42. Liston, D.J.; West, B.O. Oxochromium compounds. 2. Reaction of oxygen with chromium(II) and chromium(III) porphyrins and synthesis of a p-oxo chromium porphyrin Derivative. *Inorg. Chem.* **1985**, *24*, 1568–1576. [[CrossRef](#)]
43. Bottomley, L.A.; Neely, F.L. Stereoelectronic aspects of inter-metal nitrogen atom transfer reactions between nitridomanganese(V) and chromium(III) porphyrins. *Inorg. Chem.* **1997**, *36*, 5435–5439. [[CrossRef](#)]
44. Huang, T.; Wu, X.; Weare, W.W.; Sommer, R.D. Mono-oxido-bridged heterobimetallic and heterotrimetallic compounds containing titanium(IV) and chromium(III). *Eur. J. Inorg. Chem.* **2014**, *2014*, 5662–5674. [[CrossRef](#)]
45. Huang, T.; Wu, X.; Song, X.; Xu, H.; Smirnova, T.I.; Walter, W.; Weare, W.W.; Sommer, R.D. Ferromagnetic coupling in d1–d3 linear oxidobridged heterometallic complexes: Ground-state models of metal-to-metal charge transfer excited states. *Dalton Trans.* **2015**, *44*, 18937–18944. [[CrossRef](#)] [[PubMed](#)]
46. Super, M.; Beckman, E.J. Copolymerization of CO₂ and cyclohexene oxide. *Macromol. Symp.* **1998**, *127*, 89–108. [[CrossRef](#)]
47. Darensbourg, D.J.; Yarbrough, J.C. Mechanistic aspects of the copolymerization reaction of carbon dioxide and epoxides, using a chiral salen chromium chloride catalyst. *J. Am. Chem. Soc.* **2002**, *124*, 6335–6342. [[CrossRef](#)] [[PubMed](#)]
48. Cheng, M.; Darling, N.A.; Lobkovsky, E.B.; Coates, G.W. Enantiomerically-enriched organic reagents via polymer synthesis: enantioselective copolymerization of cycloalkene oxides and CO₂ using homogeneous, zinc-based catalysts. *Chem. Commun.* **2000**, *0*, 2007–2008. [[CrossRef](#)]
49. Nakano, K.; Nozaki, K.; Hiyama, T. Spectral assignment of poly[cyclohexene oxide-alt-carbon dioxide]. *Macromolecules* **2001**, *34*, 6325–6332. [[CrossRef](#)]
50. Super, M.; Costello, C.; Berluche, E.; Beckman, E. Copolymerization of 1,2-epoxycyclohexane and carbon dioxide using carbon dioxide as both reactant and solvent. *Macromolecules* **1997**, *30*, 368–372. [[CrossRef](#)]
51. Kooriyaden, F.R.; Sujatha, S.; Arunkumar, C. Synthesis, spectral, structural and antimicrobial studies of fluorinated porphyrins. *Polyhedron* **2015**, *97*, 66–74. [[CrossRef](#)]
52. Grancho, J.C.P.; Pereira, M.M.; Miguel, M.G.; Gonsalves, A.M.R.; Burrows, H.D. Synthesis, spectra and photophysics of some free base tetrafluoroalkyl and tetrafluoroaryl porphyrins with potential applications in imaging. *Photochem. Photobiol.* **2002**, *75*, 249–256. [[CrossRef](#)]
53. Sun, Z.-C.; She, Y.-B.; Zhou, Y.; Song, X.-F.; Li, K. Synthesis, Characterization and spectral properties of substituted tetraphenylporphyrin iron chloride complexes. *Molecules* **2011**, *16*, 2960–2970. [[CrossRef](#)] [[PubMed](#)]
54. Sugimoto, H.; Ohshima, H.; Inoue, S. Alternating copolymerization of carbon dioxide and epoxide by manganese porphyrin: The first example of polycarbonate synthesis from 1-atm carbon dioxide. *J. Polym. Sci. Part A Polym. Chem.* **2003**, *41*, 3549–3555. [[CrossRef](#)]

